

Controllable Fabrication of Spider-web-like Structured Anaphe Panda Regenerated Silk Nano-fibers/nets via Electr...

DIANA STAROVOYTOVA

Related papers

[Download a PDF Pack](#) of the best related papers 



[Silk proteins for biomedical applications: Bioengineering perspectives](#)

Felix Engel

[Silk-based biomaterials for tissue engineering](#)

Paul Hatton

[Fabrication of Silk Nanofibres with Needle and Roller Electrospinning Methods](#)

Lenka Martinová

Controllable Fabrication of Spider-web-like Structured *Anaphe Panda*

Regenerated Silk Nano-fibers/nets via Electro-netting

DULO Benson^{1,2}, WANG Na (王娜)³, LI Yan (李彦)¹, OYONDI Eric², MADARA S.Diana² and DING Bin (丁彬)¹

¹College of Textiles, Donghua University, Shanghai 200051, China

²Department of Manufacturing, Industrial and Textile Engineering, Moi University, Kenya

³State Key Laboratory for Modification of Chemical Fibers and Polymer Materials, College of Materials Science and Engineering, Donghua University, Shanghai 200051, China

Abstract:

An *Anaphe panda* silk nano-fibers/nets (NFN) membrane with attractive structures consisting of common electro-spun nano-fibers and 2-dimensional soap bubble-like structured nano-nets were successfully fabricated *via* electro-spinning/netting technology. The unique structures of NFN membranes such as extremely small diameter (<20 nm), high porosity, large specific surface area etc. and biocompatibility make this *Anaphe panda* silk NFN membrane become a promising candidate for biomedical applications. In the present study, we first used field emission scanning electron microscopy (FE-SEM) to investigate the influence of solution and humidity on nano-nets coverage and morphology. The FE-SEM images revealed that nano-net coverage area increases with increase in concentration of solution and that lower humidity has a positive influence on nano-nets formation. Moreover, the mechanical properties of the membrane were also tested and the results showed the silk NFN membrane possess a breaking stress of 3.7 MPa and breaking strain of 13.8%. For further structural elucidation, Fourier transform infra-red (FT-IR) spectroscopy was used to analyze the structural conformation changes from random coil to β -sheet in the NFN membrane which is an important factor effecting the usability of membrane. The results above thus confirm the feasibility of *Anaphe panda* NFN structures applicability in cell tissue culture and other biomedical applications.

Key words: *Anaphe panda* silk, electro-spinning/netting, nano-fibers/nets, biocompatibility

Introduction

Silk, a fibrous protein based biopolymer has gained increased interest among researchers as a biomedical material due to its array of excellent properties such as biocompatibility, slow and tunable biodegradation and superior mechanical strength [1-3]. Though *Bombyx mori* silk has been researched for centuries, noteworthy effort are being made to utilize silk from the wild silk worm species such as *Gonometa postica*, *Antherea penyi*, and *Anaphe panda* etc. [4-7]. Which have become promising source of silk for biomedical and biotechnological application. Wild silk including *Anaphe panda* fibers presented in this study show many defects including shrinkage

in hot water, poor cohesion, development of bright specks in the yarn, low dyeing ability and non-continuous fibers due to moth emergence holes^[8]. These fibers disadvantages makes nano-fibers fabrication a viable option to utilize the wild silk fibers^[9].

Recently, electro-spinning has been shown to be simple but powerful technique for the preparation of functional nano-fibers/nets (NFN) membranes^[9]. It utilizes a high voltage to induce liquid jet formation which together with electro-netting, a process involving phase separation induce splitting of small charged droplets in the high electric field resulting to formation of a three dimensional (3D) NFN. The NFN consists of conventional electro-spun nano-fibers which act as a support for the spider-web-like structured nano-nets comprising interlinked unique ultrafine 1D nano-wires^[9,10]. The resulting electro-spun nano-materials reveal numerous superb characteristics, such as remarkable size, specific surface area, flexibility in surface functionalities, and superior mechanical performance^[9-13].

The 1D nanostructures nano-nets supported by the conventional electro-spun nano-fibers in the NFN membrane have attracted a tremendous research interest due to their exceptional properties such as Steiner tree network geometry, ultrafine diameter and high porosity^[14]. Combining the intrinsic properties of NFN and the unique properties of proteineous silk polymer, it is possible for silk NFN based products to be used in biomedical areas including tissue engineering, drug delivery, and skin regeneration etc.^[12,15,16]. Modern investigations have been centered on application of various measures to control the formation of NFN membrane process in order to produce silk fibroin (SF) membranes with designed functions^[17, 18]. Zhu et al., investigated how PH and concentration of regenerated *Bombyx mori* SF aqueous solutions affects the electro-spun fibre and found out that, with the decrease in pH and concentration, the morphology of the electro-spun silk fibers changed from belt-like shape to uniform cylinder^[19]. Sachiko et al., investigated the effects of processing parameters and geometric properties on regenerated *Bombyx mori* silk and the result indicated that concentration was the most important parameters determining the size of the fibers^[20]. Studies conducted on poly (acrylic acid) and nylon-6 have shown that one of the most important parameter influencing nano-net formation is relative humidity (RH)^[21].

Few studies have been done on effect of electro-spinning parameters on the SF membrane; to the best of our knowledge no work has been done on the effects of concentration and relative humidity on *Anaphe panda* SF to produce NFN. In this study, therefore, we present an effort aiming to fabricate a controllable *Anaphe panda* NFN membrane by regulating solution concentration and relative humidity. This work is expected to enable production of NFN membrane which can add value to the biomedical fields.

1 Experimental

1.1 Materials

Cocoon nests of *Anaphe panda* were collected from Kakamega tropical rainforest, western Kenya. Sodium carbonate (Na_2CO_3), calcium nitrate tetra oxide (Ca

(NO₃)₂·4H₂O), lithium chloride (LiCl), calcium chloride (CaCl₂), methanol, ethanol and formic acid were purchased from sigma-Aldrich. And a neutral soap. Pure water was made from heal force pre-treatment device PTD-20-3 (Shanghai Convex Analytical Instrument Co., Ltd). All the chemicals were used as received.

1.2 Pretreatment

Leaves, small twigs, dusts, small insects and other foreign matters were removed from the outer surfaces of *Anaphe panda* cocoons. Cocoons nests were also dissected with a sharp blade to remove dead pupae and other insect exuvia from the inner sections. The degumming process was accomplished by a two-bath step process involving boiling the cocoons in a 5 g/L of Na₂CO₃ for 4.5 h at a temperature of 90 °C each time. After every bath, the cocoons were soaked in a neutral soap for 3 min and then rinsed twice with hot water to remove sericin. The cocoons were rinsed with distilled water and then air dried. The weight of the fibre before and after degumming was measured and recorded for evaluation of degumming efficiency. The degummed SF was then dissolved in various aqueous salt solutions and organic-salt mixtures aqueous solutions at 95 °C for 6 h. Then, the solution was filtered to remove un-dissolved debris before being dialyzed with a cellulose tubular membrane (MWCO: 3500) against a distilled water for 72 h at room temperature. The SF was eventually kept in a vacuum oven at 40°C to remove water till 6 wt% powder was obtained. The regenerated SF powder was then dissolved in 98% formic acid for 2 h under vigorous stirring to prepare 10-15 wt% solution.

1.3 Fabrication of NFN membranes

The solution was placed in a syringe needle with controlled feed rate of 0.1 mL/h regulated by syringe pump DXES-1 spinning equipment (Shanghai Oriental flying Nanotechnology Co., Ltd, China) connected to a high power voltage source. A high voltage 30 kV was applied to the needle tip resulting to continuous NFN membranes jet stream which was deposited on grounded copper plate collector placed at a distance 15 cm from the needle tip. The setup is depicted in Fig. 3a. The resulting membrane was dried in a vacuum oven for 1 h to remove the solvent.

1.4 Characterization

Gravimetric assessment of degumming efficiency was determined by the formula;

$$\text{Weight loss (\%)} = \frac{W_b - W_a}{W_b} \times 100$$

Where: W_b means weight before degumming and W_a means weight after degumming. NFN membrane morphology was examined by field scanning electron microscopy (F-SEM) (F-SEM S-4800, Hitachi Ltd, Japan). The diameter of the fibers was measured with image analyzer (adobe acrobat XI pro. 11.0.3). The mechanical properties of NFN membranes were performed on a tensile tester (XQ-1C, Shanghai New Fiber Instrument Co., Ltd., China). Fourier transform infrared (FT-IR) spectra were recorded with a Nicolet 8700 FT-IR spectrometer.

2 Results and Discussion

2.1 Efficiency of degumming

Fig. 1 shows FE-SEM images of both raw (un-degummed) silk and degummed fibers. The image of un-degummed fibre (Fig. 1a) showed a coating of white deposit (sericin) on the surface cementing the fibers together. This phenomenon is ascribed to the presence of calcium oxalate which hinders the dissolution of fibre [22]. Therefore to enable dissolution of the fibers, the coating is removed by boiling in water containing sodium carbonate and washed with a neutral soap in a process called degumming. After degumming, the fibers were examined by FE-SEM and the result showed more loosely cemented fibre and small traces of sericin gum on the fibre, as shown in Fig. 1b. The degummed fibers however, display some damage (indicated by circles on Fig. 1b) possibly due to the intensive degumming procedure. The empirical result also shows that the degumming loss efficiency expressed in terms of the total weight loss after degumming is 29.8%. The percentage weight loss reported in this paper is higher than that reported by Kabede et al. [6]. This might be attributed to increased degumming time. Though the weight loss shows higher efficiency of degumming, the traces of sericin substance observed on the fibers suggested that the degumming process did not absolutely remove all the calcium oxalate from the fibre surface.

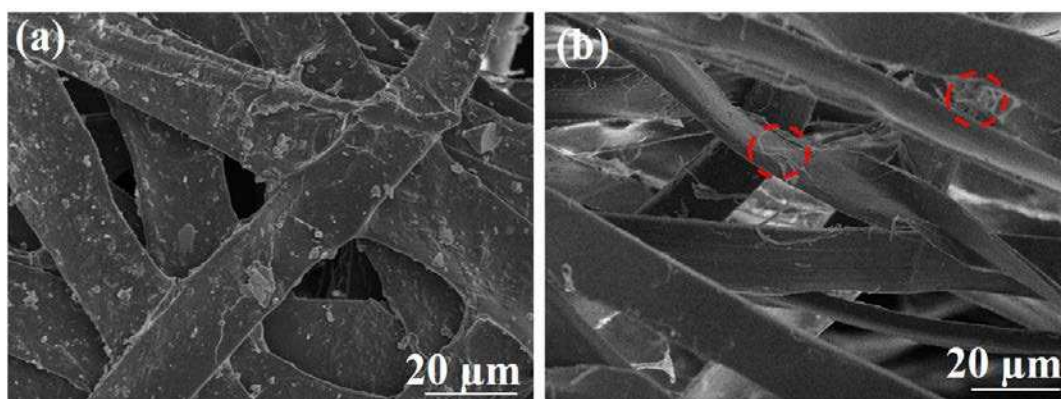


Fig. 1 FE-SEM image of *Anaphe panda* silk: (a) before degumming and (b) after degumming.

2.2 Dissolution of degummed SF

It was necessary to conduct studies as fibroin requires solubilization prior to processing it into fibrous morphologies. Previous research attempts have shown that *Anaphe panda* silk gels during dissolution and is difficult to handle with lower solubility [23]. As there is no comprehensive information regarding the dissolution of *Anaphe panda* SF, a number of solvent systems were investigated. Table 1 shows solubility of fibroin in different aqueous salt-organic mixture and aqueous salts at various concentrations.

From Table 1, $\text{Ca}(\text{NO}_3)_2 \cdot 4 \text{H}_2\text{O}$ melt showed the highest solubility. Though the solubility is optimal and higher than any other reported work, the fibroins were however not fully dissolved. This might be due to the traces of calcium oxalate which remained after degumming. $\text{Ca}(\text{NO}_3)_2 \cdot \text{H}_2\text{O}$: Me OH (1:4:2) and LiBr salt also showed relatively high solubility. However this result is different from one conducted by Addis et al., where calcium nitrate was not included in the salt solvent evaluation

and reported higher solubility using LiBr salt^[23]. Lithium chloride and calcium chloride did not dissolve the fibre. The result shows consistency with findings of Mhuka et al., on dissolution of *Gonometa Postica* and *Gonometa Rufobrunnae* wild silk^[4].

Table 1 Solubility of *Anaphe panda* silk in various solvents.

Solvents	Concentrations	Solubility (%)
LiBr	7M	not soluble
LiBr	9.5 M	49.33
LiCl	7M	not soluble
LiCl	9.5 M	not soluble
CaCl ₂	7M	not soluble
CaCl ₂	9.5 M	not soluble
Ca(NO ₃) ₂	7M	not soluble
Ca(NO ₃) ₂	9.5 M	11.90
Ca(NO ₃) ₂ ·4 H ₂ O	Melt	88.00
LiCl:EtOH:H ₂ O	4:4:1	not soluble
LiBr:EtOH:H ₂ O	4:4:1	not soluble
CaCl ₂ :EtOH:H ₂ O	1:2:8	not soluble
Ca(NO ₃) ₂ :H ₂ O:MeOH	1:4:2	77.50

Except for Ca (NO₃)₂:H₂O: Me OH (1:4:2), aqueous salt-organic solvent has little dissolution effect on *Anaphe panda* silk. The dissolution phenomenon could be possibly explained by the fact that inter and intra-molecular silk hydrogen network bonds are ruptured by solvent's anions nucleophilic attack on their electrophilic centers. Anions of lower charge density increase protein solubility by interacting more with amide, hydroxyl and amino groups in the protein more than anions of higher charge density^[24]. Aqueous solution of NO₃⁻ and Br⁻ are more nucleophilic than Cl⁻ thus has shown higher protein solubility. Aqueous salt-organic (methanol or ethanol) solvent mixture did not improve the solubility of the fibroin but instead some salts like LiBr lost their solubility power which agrees with the report by Mhuka et al.^[25]. This however, might be explained by a reasoning that water miscible organic solvents lowers the dielectric constant of salt solutions thus dipole-dipole and charge-dipole interaction reduction resulting to drop in solubility. Further analysis may be required to fully explain the occurrence.

2.3 Electro-spinning/Netting (ESN)

The image of the resulting silk membrane at various concentration and humidity are shown in Fig. 2(b-d and g). The morphology shows an interesting structure comprising of ultra-fine nano-wire supported by conventional electro-spun fibre. The 1D nano-wires are interlinked into a spider-web-like net structure. The nano-nets exhibited varied coverage rate (up to 97%) depending on the conditions variations. The high resolution FE-SEM image showed a diameter range between 10-20nm for nano-nets, while that of nano-fibers averages diameter was 250 nm (Fig. 2e and f).

The nano-nets are formed through a process of ESN, which could be explained by a mechanism of phase separation of charged droplets generated during ESN^[9]. From Fig. 2a, at a high voltage, the charged droplet undergoes significant deformation stretching to become thin liquid droplets, which further undergoes phase separation with the domain dominated solvents forming pores. In view of the minute size of the droplets, however, the surface tension and columbic repulsion could play a role in keeping the droplets spherical in shape, instead of further distortion^[11, 26].

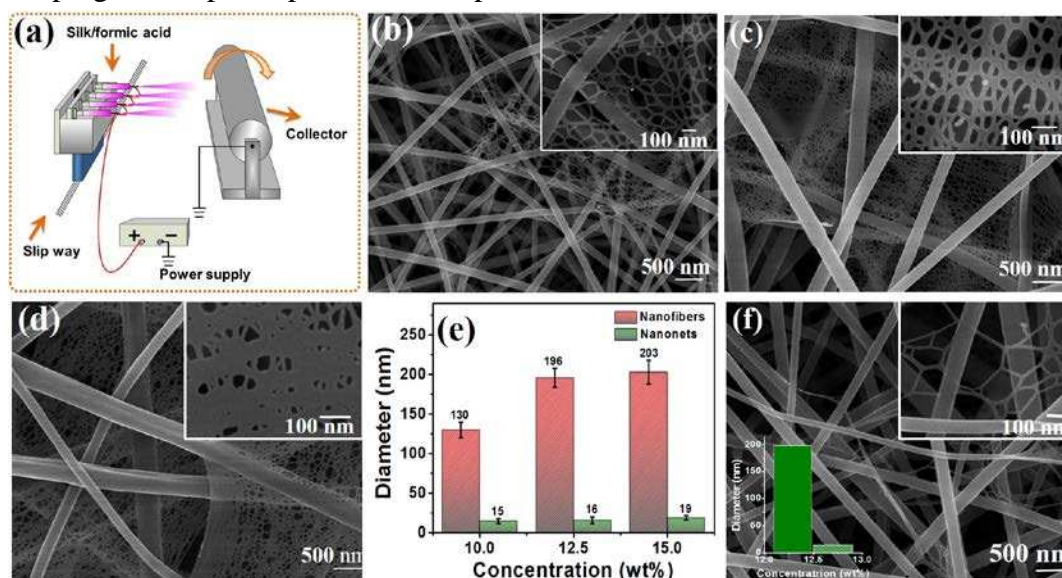


Fig. 2 (a) Schematic set up illustrating NFN membrane formation mechanism during ESN process. FE-SEM images of silk membrane formed with varying concentration and RH. (b) (10 wt% at RH 25±5%), (c) (12.5wt% at RH 25±5%), and (d) (15 wt% at RH 25±5%). (e) Fibre diameters variation with solution concentration. (f) FE-SEM images of silk membrane formed by 12.5 wt% at RH 40±5%.

Research has proved that morphology and structure are influenced by electro-spinning parameters^[26]. As presented in Fig. 2, we investigated the effects of the ESN parameters on the structure and morphology of silk NFN membranes by systematically controlling the ESN parameters. The NFN silk membranes morphologies formed by varying solution concentration 10, 12.5, and 15wt%. As shown by FE-SEM are presented in Fig. 2 b-d respectively, while Fig. 2f shows the morphological image at RH of 40±5% for same solution concentration of 12.5 wt%.

It was observed that increasing the solution concentration increases the diameter of nano-wire and nano-fibers, as shown in Fig. 2e. However the pore width of the nano-nets were reduced. The finding is in agreement with the results reported by Ding et al.^[10]. This could be as a result of increase in viscosity of the solution hindering the jet thinning thus incomplete separation of nano-wires. Fig. 2f shows FE-SEM images of silk NFN membranes produced at RH of 40±5% with 12.5 wt% concentration. It reveals the presence of NFN morphology; this confirms the possibility of forming silk NFN at higher humidity. Though in comparison with NFN formed at lower humidity and same solution concentration Fig. 2c, the morphology shows that the nano-wires reduces in diameter in agreement with observation made by Zong and co-workers^[21]. The decrease in fiber diameter could be attributed to the slower solidification

process of the jets resulting in a longer time of elongation of the jet, thus producing thinner nano-fibers.

Fig. 2b-d also shows an important characteristic of NFN membranes controllable coverage rate, which is defined as the area ratio of nano-nets to the whole membrane. Higher area coverage is important for efficiency of NFN applicability. The FE-SEM indicates that nano-net coverage increases with an increase of concentration however, the pore size decreases with increase in concentrations Fig. 2b-d. The reduced coverage at lower concentration could be possible due to low solution viscosity resulting to faster evaporation for phase separation to occur thus formation of more conventional nano-fibers. Further increasing the concentration can reduce electrostatic forces on the droplets, which may hinder stretching of the jets negating favorable formation of completely split nano-nets thus reduced pore size. Therefore, the concentration and humidity plays an important role in controlling the coverage rate of nano-nets.

2.4 Mechanical properties

Fig. 3a and b presents mechanical failure (stress-strain) graphs of silk at different stages in ESN process. Fig. b shows failure mechanism of NFN silk membrane formed at solution concentration of 12.5 wt% and RH of $25 \pm 5\%$ believed to be the optimal condition for NFN membrane formation. Fig. 3a showed that raw silk has a higher breaking strength (300 MPa), while degummed silk showed 135 MPa. The higher breaking strength could have been due to the gummy sericin which forms a composite like structure with the fibre. When sericin was removed during degumming process, a reduction in strength was observed. The reduction in strength was higher than expected which could be attributed to the severity of the degumming process and destruction of the fibers as depicted in Fig. 1b. In Fig. 3b, the initial part of the stress-strain curve shows a higher modulus which on further stretching gradually reduces in magnitude before snapping. Between the two phases of modulus is a pseudo-yield point. This graph differs from that of Ayusdet e et al., in which there was no nano-net in the membranes ^[27]. Thus could be attributed to the presence of the unique NFN combination in the membrane. This phenomenon may be explained by a two-step failure mechanism as depicted in Fig. 3c. The NFN membrane possess nano-wire net supported by common nano-fibers which probably could exhibit different transformation characteristics in tensile loading. At initial loading, the numerous nano-wire nets are likely to offer higher resistance to applied force thus higher initial modulus (1.2 MPa). At pseudo-yield point, it is believed that the nano-wire nets have broken up, the main common fibers tends to slip-apart giving a nonlinear part of the graph. The curve then changes to a quasi-linear final part due to individual elongation of the aligned conventional fibers results to a final modulus of 0.1 MPa. Finally, the fibers undergoes reduction in cross-sectional area leading to less number of fibers in the cross-section hence failure of the membrane at braking stress of 3.7 MPa and 14% elongation at break. This indicates good mechanical strength thus making silk fibre suitable for its intended application.

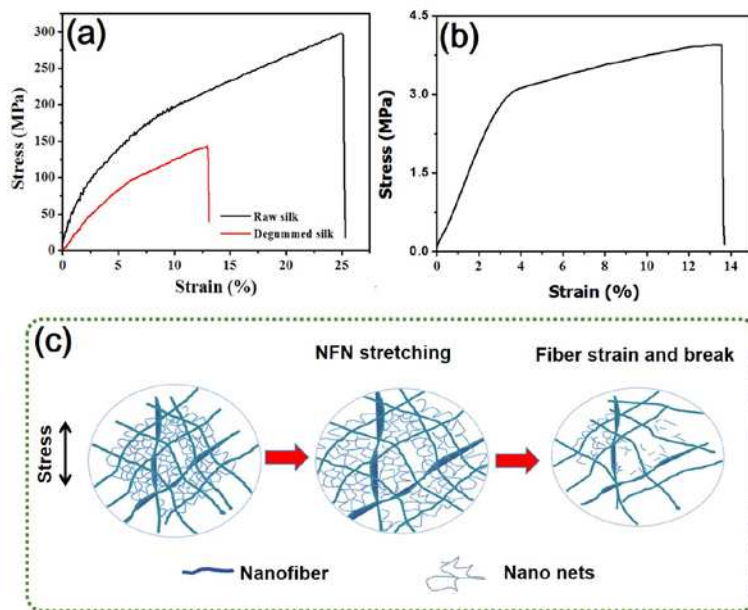


Fig. 3 stress-strain curve for (a) raw and degummed silk, (b) NFN membranes, and (c) two step failure mechanism of NFN membranes.

2.5 Structural conformation

The FTIR spectroscopy was used to follow the conformational changes that occur in the three silk fibrous substances (pristine, degummed, and NFN). By analyzing the infrared spectrum, the structural conformation of Silk Fibers can be determined, depending on the wave number and peaks location of the absorption bands of amides I, II and III. The infrared spectra of the fibers are shown in Fig. 4. Simultaneous presence of the two major conformations: random coils (silk I) and β -sheet (silk II) were observed. The image showed no major difference in the key bands. However, the bands display significant changes in peak intensities signifying variations in secondary structure. From Fig. 3, absorption bands are presented at $1,650\text{ cm}^{-1}$ (amide I) and $1,520\text{ cm}^{-1}$ (amide II), corresponding to the SF silk II structural conformation (β -sheet). Other absorption bands were observed at $1,530\text{ cm}^{-1}$ (amide II) and $1,230\text{ cm}^{-1}$ (amide III), which are characteristic of the silk I conformation (random coil and α -helix).

The result shows higher conformational increase in β sheets contents in the NFN membrane depicted by the increase in peak intensities; the β sheets structure confirms good applicable mechanical properties. Moreover the β sheets structure can be increased in the membrane through post spinning treatment further increasing mechanical strength and insolubility of the membrane in water^[28]. The sheets peak intensities variation in the electro-spun silk shows that there is structural change in the conformation of the silk fibers. These structural behaviors are important since they can be considered to be available for the control of solubility in water depending with the environmental condition of membrane application.

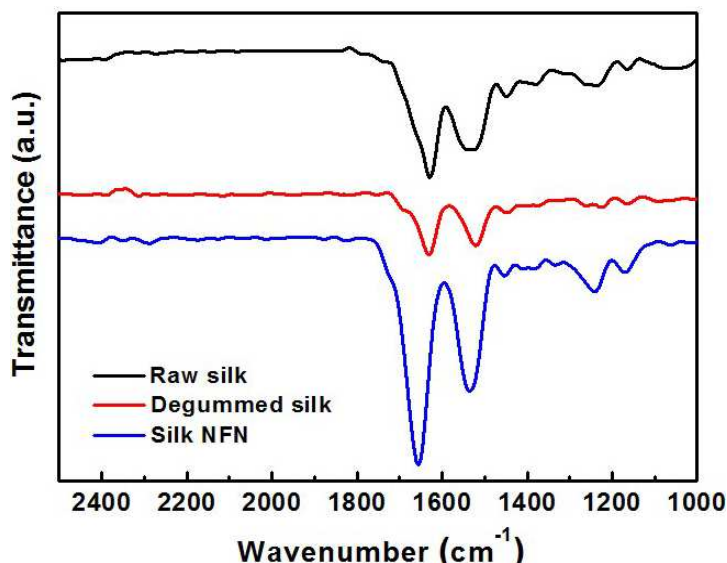


Fig.4 FT-IR image of pristine, degummed, and NFNApache Panda silk membranes.

4. Conclusion

Spider-web-like structured NFN were successfully generated from *Anaphe Panda* silk via ESN. Proper degumming of the wild *Anaphe panda* species silk is necessary to enable dissolution of the fibroin. The traces of sericin which remained after degumming reduced efficiency of dissolution. Degummed *Anaphe panda* silk can be better dissolved by $\text{Ca}(\text{NO}_3)_2 \cdot \text{H}_2\text{O}$ melt. May be by increasing agitation and/or degumming temperature, higher solubility could be realized. Further work should be done to reveal the optimum degumming and dissolution conditions. By ESN, a fascinating 3D structure consisting of 2D spider-web-like nano-nets supported by conventional electro-spun nano-fibers could be finely controlled. NFN morphology was found to be greatly affected by electro-spinning solution concentration and ambient relative humidity. Formation of NFN structure was also found to influence the mechanical behavior of the fibers. The structural conformation indicated existence of a dimorphic structures of both random α and β -sheets in the NFN membrane hence has controllable water solubility properties. The higher peak intensity of β -sheets indicates better mechanical properties. With the NFN membrane of Silk showing advantage of large specific-surface area, high porosity, large stacking density, unique Steiner tree networks geometry, good mechanical properties, coupled with the known novel tunable biodegradability and biocompatibility properties, *Anaphe panda* silk NFN membranes provide a potential biomedical material.

References

1. Mondal K. The silk proteins, sericin and fibrion in silkworm, *Bombyx mori* Linn., a review. *Caspian Journal of Environmental Sciences*. 2007, 5(2):63-76.
2. Vepari C, Kaplan DL. Silk as a biomaterial. *Progress in Polymer Science*. 2007, 32(8-9):991-1007.
3. Pritchard EM., Normand V, Hu X, et al. Encapsulation of oil in silk fibroin biomaterials. *Journal of Applied Polymer Science*. 2014, 131(6):345-357

4. Mhuka V, Dube S, Nindi MM, et al. Fabrication and structural characterization of electrospun nanofibres from *Gonometa Postica* and *Gonometa Rufobrunnae* regenerated silk fibroin. *Macromolecular Research*. 2013, 21(9):995-1003.
5. He J X, Cheng Y, Cui S. Preparation and characterization of electrospun *Antheraea pernyi* silk fibroin nanofibers from aqueous solution. *Journal of Applied Polymer Science*. 2013, 128(2):1081-1088.
6. Kebede AT, Raina SK, Kabar JM. Structure, composition, and properties of silk from the African wild silkmoth, *Anaphe panda* (Boisduval) (Lepidoptera: Thaumetopoeidae). *International Journal of Insect Science*. 2014, 6(4038):9-14.
7. Teshome A, Onyari JM, Raina SK, et al. Mechanical and thermal degradation properties of silk from African wild silkmoths. *Journal of Applied Polymer Science*. 2013, 127(1):289-297.
8. Kato H, Hata T, Takahashi T. Characteristics of wild silk fibers and processing technology for their use. *Jarq-Japan Agricultural Research Quarterly*. 1997, 31(4):287-294.
9. Wang X F, Ding B, Sun G, et al. Electro-spinning/netting: A strategy for the fabrication of three-dimensional polymer nano-fiber/nets. *Progress in Materials Science*. 2013, 58(8):1173-1243.
10. Ding B, Li C R, Miyauchi Y, et al. Formation of novel 2D polymer nanowebs via electrospinning. *Nanotechnology*. 2006, 17:3685-3691.
11. Hu J P, Wang X F, Ding B, et al. One-step electro-spinning/netting technique for controllably preparing polyurethane nano-fiber/net. *Macromolecular Rapid Communications*. 2011, 32(21):1729-1734.
12. Lin L, Perets A, Harel Y, et al. Alimentary 'green' proteins as electrospun scaffolds for skin regenerative engineering. *Journal of Tissue Engineering and Regenerative Medicine*. 2013, 7(12):994-1008.
13. Hsieh Y L. Nanofibrous membranes from aqueous electrospinning of carboxymethyl chitosan. *Nanotechnology*. 2008, 19(12):125707.
14. Nasser AM, Barakata B, Muzafar A, et al. Spider-net within the N6, PVA and PU electrospun nanofiber mats using salt addition: Novel strategy in the electrospinning process. *Polymer*. 2009, 50(18):4389-4396.
15. Elakkiya T, Malarvizhi G, Rajiv S, et al. Curcumin loaded electrospun *Bombyx mori* silk nanofibers for drug delivery. *Polymer International*. 2014, 63(1):100-105.
16. Lv J, Chen L, Zhu Y, et al. Promoting epithelium regeneration for esophageal tissue engineering through basement membrane reconstitution. *ACS Applied Materials & Interfaces*. 2014, 6(7):4954-4964.
17. Chutipakdeevong J, Ruktanonchai U R. Process optimization of electrospun silk fibroin fiber mat for accelerated wound healing. *Journal of Applied Polymer Science*. 2013, 130(5):3634-3644.
18. He J X, Cui Y, Li P, et al. Preparation and characterization of biomimetic tussah silk fibroin/chitosan composite nanofibers. *Iranian Polymer Journal*. 2013, 22(7):537-547.
19. Zhu J, Zhang Y, Shao H, et al. Electrospinning and rheology of regenerated *Bombyx mori* silk fibroin aqueous solutions: The effects of pH and concentration.

Polymer. 2008, 49(12):2880-2885.

20. Sachiko S, Milind G, Jonathan A, et al. Michael Micklus. Regeneration of Bombyx mori silk by electrospinning-part 1: Processing parameters and geometric properties. Polymer. 2003, 44 (19):5721-5727.

21. Zong X, Kim K, Fang DF, et al. structure and process relationship of electrospun bioabsorbable nanofibre membranes. Polymer. 43 (2002), pp. 4403-4412

22. Gheysens CA, Raina S, Vollrath F, et al. Demineralization enables reeling of wild silkmoth cocoons. Biomacromolecules. 2011, 12(6):2257-2266

23. Addis KT, Raina SK. Dissolution properties of silk cocoon shells and degummed fibers from African wild silkmoths. Pakistan journal of biological sciences: PJBS. 2013, 16(20):1199-1203.

24. Kelemen L, Fábrián L, Taneva SG, et al. Interfacial water structure controls protein conformation. Journal of Physical Chemical B. 2007, 111(19):5344-5350.

25. Mhuka V, Dube S, Nindi MM. Chemical, structural and thermal properties of Gonometa postica silk fibroin, a potential biomaterial. International Journal of Biological Macromolecules. 2013, 52:305-311.

26. Wang N, Wang X., Ding B, et al. Tunable fabrication of three-dimensional polyamide-66 nano-fiber/nets for high efficiency fine particulate filtration. Journal of Materials Chemistry. 2012, 22(4):1445-1452.

27. Ayutsede J, Gandhi M, Sukigara S, et al. Regeneration of Bombyx mori silk by electrospinning. Part 3: Characterization of electrospun nonwoven mat. Polymer. 2005, 46(5):1625-1634.

28. Tanaka C, Asakura T. Synthesis and characterization of cell-adhesive silk-like proteins constructed from the sequences of Anaphe silk fibroin and fibronectin. Biomacromolecules. 2009, 10(4):923-928.